

DESOLINATION PROJECT sCO₂ AXIAL EXPANDER DEVELOPMENT

Lorenzo Cosi
Baker Hughes
Nuovo Pignone
Firenze, Italia

Andrea Paggini
Baker Hughes
Nuovo Pignone
Firenze, Italia

Tommaso Diurno
Baker Hughes
Nuovo Pignone
Firenze, Italia

Andrea Nenciolini
Baker Hughes
Nuovo Pignone
Firenze, Italia

Lorenzo Lunghi
Baker Hughes
Nuovo Pignone
Firenze, Italia

ABSTRACT

sCO₂ energy conversion cycles technology development is reaching the MW-scale cycle demonstration phase. At the moment of this abstract writing, the STEP plant is going through the different phases of commissioning and has already produced electrical power. Other demonstration projects are reaching the end of the design phase and forecast a commissioning start in 2026. Nuovo Pignone Baker Hughes is part of the Desolination project consortium. Desolination project aims to decarbonize the desalination process in arid regions by demonstrating in a real environment the efficient coupling of a concentrating solar power plant to a direct osmosis desalination system. The sCO₂ cycle involved in this process is a Transcritical evolving a blended CO₂ mixture optimized to enable condensation in hot ambient temperature areas.

Nuovo Pignone contributes to the Desolination project developing the pump and the expander of the sCO₂ cycle. Expander development has reached the completion of the detailed design phase and the procurement of long lead material has started. This paper will provide a comprehensive overview of the expander development process, from conceptual design through to detailed design, displaying the key technology challenges peculiar of sCO₂ expanders and illustrating the engineering methodologies applied to optimize the expander design.

INTRODUCTION

Desolination project, an EU-funded project, aims at demonstrating a combined desalination and sCO₂ power conversion system based upon solar energy source (see Figure 1). A detailed description of the power cycle thermodynamics and layout is reported in Morosini et al. [7]. The sCO₂ cycle is based upon a binary fluid mixture that has been designed to enable condensation in hot area as described in Abdeldayem et al. [1]. Demonstrator plant will be constructed in King Saud University in Riyadh, Saudi Arabia and it will be integrated with an existing CSP Air Brayton cycle as illustrated in Figure 2. The plant components will be installed in standard containers (see Figure 3)

ahead of the field installation in order to limit the civil works at site and reduce the overall installation schedule.

The sCO₂ expander is one of the most critical equipment of the Desolination plant. Several authors have illustrated their approach to the design of sCO₂ expanders for other power cycles highlighting the specific challenges that characterize these class of expanders and the conceptual solution adopted to optimize their design. Bidkar et al. have presented the design of a 50 MWe and a double flows 450 MWe sCO₂ expander. Other authors including Moore et al. [8] have illustrated the development of the STEP 10 MWe sCO₂ expander which is currently under commissioning at SwRI. Glos et al. [3] have described the design of the 2MW Carbosola project sCO₂ axial expander. Abdeldayem et al. [1] have presented the design of the 130 MW axial expander developed in the frame of the Scarabeus project (see the expander cross section in Figure 4) highlighting several aspects of the design including a flow path optimization process that led to the selection of a 14 stages configuration, the exhaust section CFD optimization, the last stage aeromechanical assessment, the detailed thermal analysis of the unit and the Rotordynamics analysis.

The specific expander design conditions of the Desolination project are the following:

- Inlet Conditions: 200 bar and 550°C
- Exhaust Pressure: 93 Bara
- Mass Flow: 27 kg/s
- Process fluid: 82% CO₂-18% SO₂ (molar basis).

It is remarked that the conditions above are the result of a tradeoff between the need to have a demonstrator sufficiently representative of possible industrial scale up and the need to limit the cost of the demonstrator itself.

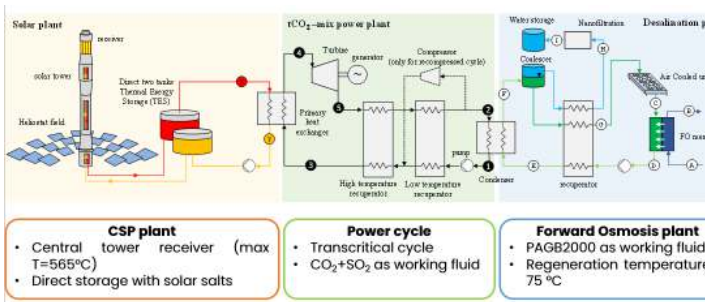


Figure 1: Desalination plant concept



Figure 4: Scarabeus Project 130 MW sCO₂ expander

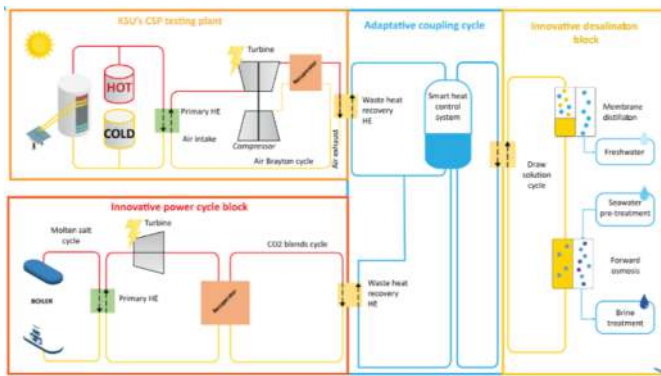


Figure 2: Desalination demonstrator plant layout



Figure 3: Containerized plant component example

SCO₂ EXPANDERS TECHNOLOGY CHALLENGES

sCO₂ expander technology design challenges have been widely illustrated in Abdeldayem et al. [1] where the lack of a consolidated supply chain for the major components (casing castings and rotor forging) driven by materials compatibility with blended sCO₂ fluid has been highlighted as one of the most challenging aspects for the expander manufacturing. This issue is partly mitigated in Desalination program where the smallest size of the machine opens up to a wider set of manufacturing options that will be illustrated later in this article.

Marion et al. [2] have illustrated that a risk factor in sCO₂ expander (independently from the blend of the fluid) is the management of the thermal gradient in the rotor and in the casing between the Dry Gas Seal (DGS) area (that shall be kept below 200°C) and the rotor and casing parts exposed to the inlet hot fluid. Management of the thermal transient stress associated to this temperature mis-match is eventually posing challenges to the design of the shaft end area as reaching adequate Low Cycle Fatigue (LCF) capability becomes not obvious. Also the aeromechanics design of the rotating blades is highlighted, in the same paper, as a significant challenge and an optimization of the inlet and exhaust plenum aimed at minimizing flow distortion is suggested.

Glos et al. [3] remark that a particular attention shall be paid to the aerodynamic design since the fluid and cycle characteristics make it more sensitive to any pressure loss compared to the traditional steam cycle, this aspect is also illustrated in this paper (see Figure 5) along with the inlet aero optimization that has been performed to address this challenge. The same paper also highlights rotordynamics design challenge associated with the highest fluid destabilizing forces.

DGS INTRODUCTION

One of the most significant technical challenges of sCO₂ power cycle is the shaft-end sealing technology. Indeed, labyrinth seals, widely used in steam turbine applications, are not suitable due to extremely high operating pressure of these

expanders which leads to high leakages and consequently cycle efficiency penalty. The latter is due to specific properties of the $s\text{CO}_2$ that has to be reintegrated in the loop. The leaked $s\text{CO}_2$ has to be recompressed in gaseous state, contrary respect to steam turbine where it is recondensed and pumped.

In order to reduce the shaft-end leakages the Dry Gas Seal (DGS) are recognized as key enabling technology for closed loop $s\text{CO}_2$ cycles. The working mechanism of this dynamic seal is based on a few microns gap between rotating and static parts maintained with a balance of hydrodynamic and elastic force, with extremely low leakages. The installation of DGS in the expander presents several challenges: high pressure, high temperature and high speed. In the current state-of-the-art the operating conditions of these seals are, indeed, limited in temperature due to internal secondary sealing elements, typically made in elastomeric or polymeric compound, with a maximum allowable temperature of 220-250 °C. This temperature limit is hard to guarantee during expander operation due to significant internal viscous heat generated in the few microns gap, in addition to the heat transferred by conduction from the hot region of the expander. At this regard, a thermal management system seems essential to cool down the seal. Alternatively, Nielson et al [14] proposed a novel high temperature DGS, with a maximum allowable temperature of 500 °C but with additional leakage penalty respect to traditional DGS. However, at the author's knowledge, this technology is not yet available on a commercial scale.

The maximum allowable temperature is not the only challenge for the DGS design, at this regard, Cich et al. [15] have carried out an experimental campaign in a $s\text{CO}_2$ DGS test bench aimed at investigating the seal behavior during start-up and shutdown. This study highlights the potential formation of dry ice in the DGS vents. This phenomenon is caused by Joule-Thomson effect through the seal with the consequent phase change from gas to solid, which can lead to mechanical failure of the seal. Several publications can be found in literature focused on exploring the operation of the DGS in $s\text{CO}_2$ environment [16], [17],[18], [19], [20], [21][22]. Recently, Wilkes et al. [23] showed the criticalities in the design of $s\text{CO}_2$ with 720 °C and 275 bar as maximum temperature and pressure with commercial DGSs as shaft-end sealing technology with a dedicated cooling system. The expander has been operated for over 100 h with a maximum temperature limited to 600 °C.

In the light of all the mentioned criticalities, a deep knowledge of thermal behavior of the seal is essential for the design of this component. In this work, a Whole Engine thermal Model (WEM) is presented to design the expander, with a detailed thermal resolution of the shaft-end area. The thermal model has been built by considering the findings proposed by Refanelli et al. [24], where a segregated conjugate heat transfer numerical procedure has been presented and validated with experimental data provided by Flowserve on a $s\text{CO}_2$ DGS rotating test rig [25]. A similar approach has already been presented by the authors for the design of $s\text{CO}_2$ SCARABEUS expander [1].

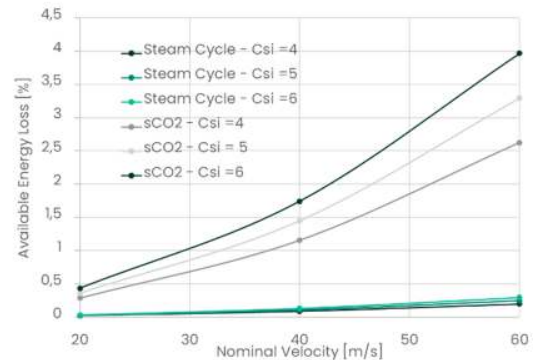


Figure 5: Inlet system losses impact on available expander energy

EXPANDER ARCHITECTURE

The small size of the Desolination plant is such that a radial flow-path technology for the expander would have been the natural choice. Nonetheless, targeting the industrial sizes foreseen for the $s\text{CO}_2$ technology, it has been decided to pursue an axial design, so as to have a demonstration plant as representative as possible of the full-scale plants.

The first thermodynamic cycle conceived for Desolination resulted in a volumetric flow at expander inlet very small ($< 0.1 \text{ m}^3/\text{s}$): an axial expander designed for those conditions was below the minimum size manufacturable in the Baker Hughes (BH) facilities and exploiting the BH supply chain. Due to this constraint, the cycle conditions and the demonstration plant size have been reconsidered, increasing the volumetric flow at inlet up to $0.2 \text{ m}^3/\text{s}$, which has been judged the minimum possible for BH to design and manufacture an axial flow-path expander.

It is worth remarking that the limit of $0.2 \text{ m}^3/\text{s}$ has been established with a tradeoff between the conflicting goals to have the demonstration plant as representative as possible of the industrial scales and not to increase too much the size of the demonstrator itself: in this regard, the peripheral speed of the rotor at average radius ($\sim 130 \text{ m/s}$) has been chosen pretty much below the limits imposed by rotor material, which would be the primary design intent aimed to minimize the number of axial stages necessary to manage the enthalpy drop. Increasing the rotating speed maintaining the same hub diameter, in fact, would have either reduced too much the flow coefficient of the stages or required a corresponding increase of the mass flow, implying a further oversize of the demonstrator. Conversely, achieving the peripheral speed increase in a rotor having a reduced hub diameter would have avoided the negative effects just mentioned but would have implied an expander size below the BH manufacturing capability.

The architecture of the expander has been chosen having in mind not only the specific conditions of the demonstrator, which are not extreme, but also the possible conditions foreseen for industrial sizes: although the inlet pressure and temperature of Desolination, 200 bar and 550°C , could have been targeted with

different design choices, the final architecture has been conceived to be suitable for higher process conditions, up to 250 bar and 620°C, which seem of interest for real industrial applications.

The design employs an external casing barrel type, aimed to minimize radial deformations, which is subjected to the thermodynamic conditions at the exhaust of the expander. The inlet fluid (split in two) is admitted into an inner casing, accommodating the statoric blades of all the 5 stages, which is split into two halves in a plane containing the machine rotational axis. The external casing is bolted to a closing flange in a plane perpendicular to the machine axis.

It has been remarked in that sCO₂ cycles are extremely sensitive to pressure losses across the inlet valves: this is mitigated by reducing as much as possible the fluid velocities at inlet (targeting values in the order of 20-30 m/s, well below the typical numbers encountered in steam turbines, for instance) and this can be better achieved by splitting the flow in two, since the radial dimension of the casing can be kept smaller and, moreover, the symmetric design is beneficial to minimize thermal distortions. Although the volumetric flow of Desolination is such that the inlet fluid velocities would be low enough even with a single inlet, the philosophy to have a design as representative as possible of the full-scale has been pursued.

Rotor is a single forging with integral blades realized by EDM machining. The reason is that, with separate rotor blades, whichever is the root employed (either a T-root or, even, a more radially compact firtree), the consequent reduction of the stiffness diameter of the rotor would have negatively impacted the rotor-dynamic stability.

FLOW PATH OPTIMIZATION

As it has been already mentioned in the previous chapter, particular attention must be paid to the aerodynamic design of the entire sCO₂ turbine due to several criticalities and in particular because of the increased flow losses due to the fluid high density. In order to maximize the overall efficiency, detailed optimizations have been carried out on both the stationary and rotating components: Inlet volute, nozzles and blades and the diffuser. With the purpose to determine the final blades count and the relative flutter instability behavior related to the possible high density fluid-structure interactions, a deeply detailed aeromechanic analysis have been performed even if it will not be analyzed within this article but in a dedicated later one.

Volute: The inlet flow is split into two halves (see Figure 6) and the geometry has been designed aiming to reduce the total pressure losses as much as possible along the entire scroll and to convey the fluid mixture towards the first statoric row in the most efficient, regular and well tangentially distributed way in terms of mass low rate and swirl.

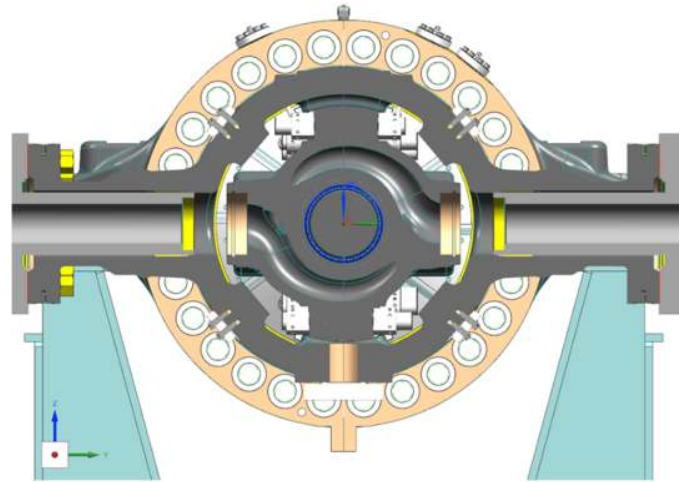


Figure 6: Inlet system configuration

To simulate and evaluate the aerodynamic performance of the volute, a 3D viscous CFD analysis have been carried out: the model was comprehensive of the entire scroll and of the first full annulus nozzle row (see Figure 7).

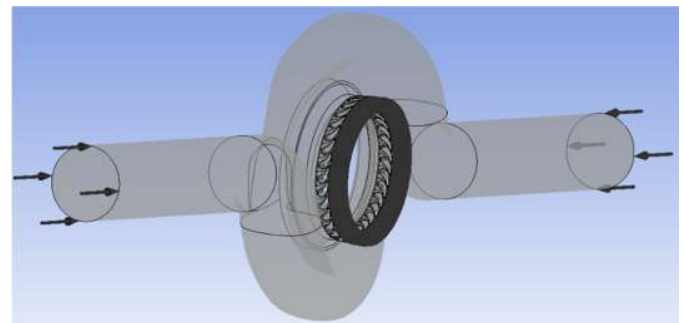


Figure 7: Inlet system CFD analysis domain

The resulting model is constituted by around 60 Millions elements (it takes around 4 days and 17 hours to satisfy convergence criterion running upon 160 CPU) but it is well suited to provide accurate and reliable results: the boundary layer areas are modeled with 30 layers within the inflation with a proper growth rate capable to match a sufficiently low average y^+ (within 5 and 10) on the wall surfaces (see mesh details in Figure 8 below). Real gas model has been implemented utilizing Refprop library.

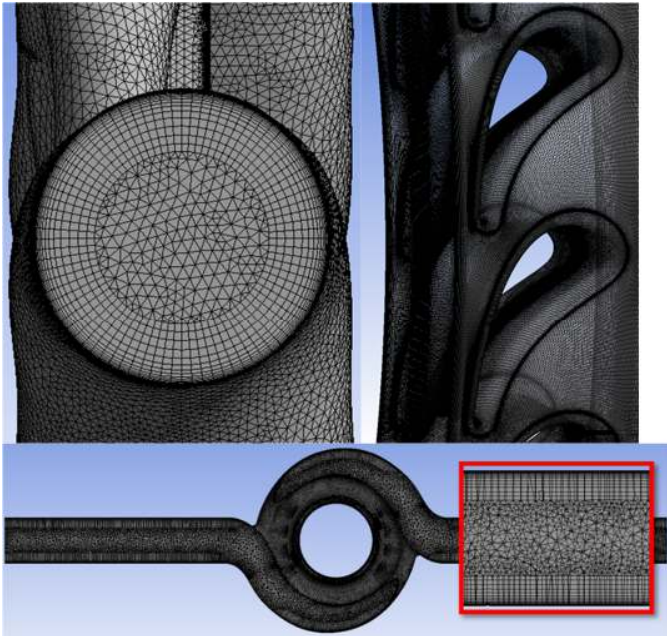


Figure 8: Inlet system CFD analysis mesh details

The CFD model adopted is a Reynolds averaged Navier-Stokes simulation with the shear stress transport (k-w SST) turbulence model as it has been proven to be a suitable one for this kind of applications. With the purpose to be as accurate as possible in the thermodynamic properties evaluations, a real gas model has been chosen. With the purpose to evaluate the volute behaviour, we could have directly modeled it as perfect gas considering that the compressibility factor is pretty much close to the unit (3% difference) but the real gas adoption allowed also to check in detail any differences in terms of flow function with different nozzle configuration.

Results related to the design point show that the scroll doesn't present any relevance of separation or recirculation once the flow enters inside the toroid: the picture below represents the tangential velocity plot along the volute inlets midplane perpendicular to the turbine rotational axis.

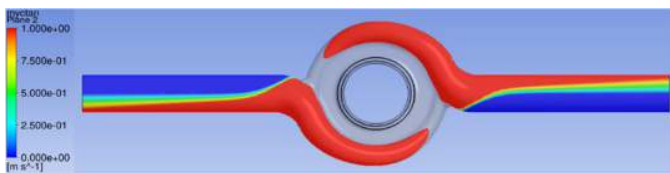


Figure 9: Inlet system tangential velocity plot

The overall inlet volute performance, in terms of pressure losses, demonstrates a good behavior: having defined a dimensionless total pressure losses coefficient CSI as below, it turns out to be 0.955 (the numerator is defined as the overall total pressure loss between inlet and outlet section while at the denominator there is the inlet kinetic component).

$$\xi = \frac{P_{Tin} - P_{Tst}}{P_{Tin} - P_s}$$

In order to have an optimized blades design it is important to determine how is the volute discharge flow distribution along the 360 degrees and, in particular, mass flow rate and swirl have been checked upon an immediate upstream first nozzle section. As it is observable from the first chart below, the inlet dimensionless mass flow rate of each vane is pretty constant and a similar consideration can be done about the first nozzle inlet swirl: the averaged incidence angle is around 40 degrees.

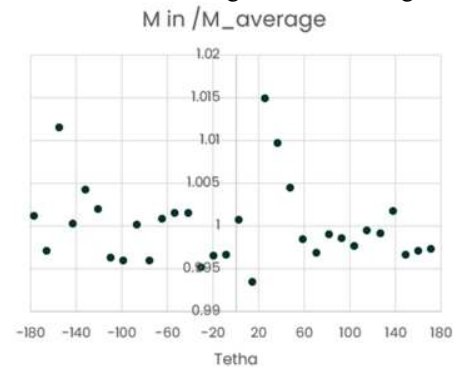


Figure 10: Normalized mass flow distribution at first stage nozzle leading edge

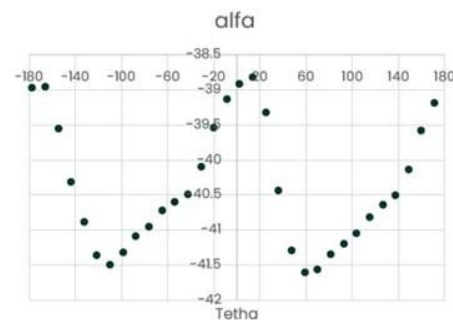


Figure 11: Flow angle distribution at first stage nozzle leading edge

Blades: the flowpath design started from a high efficiency reaction blade master model (for both nozzles and rotors) which has a predefined airfoil and can be customized in terms of stagger angle, chord length and blade height to target the optimal condition which is ideally at degree of reaction of 0.5, Load Coefficient (see the definition below) around 2 and a Flow Coefficient (see definition below) of 0.34. Due to strict constraints in terms of rotordynamics, which has limited the maximum shaft length, the total enthalpy drop has been split in a total of 5 stages with a resulting load coefficient slightly higher for each stage. As anticipated in the expander architecture chapter, the rotordynamics constraint also led to select a rotor with integral blades realized by EDM machining.

$$\psi = \frac{\Delta H_{is}}{\frac{u^2}{2}}$$

$$\varphi = \frac{C_x}{u}$$

The fluid high density results in a very low volumetric mass flow rate at inlet entrance which would lead to blades low aspect ratio compared to classical steam turbines design. This low aspect ratio has an impact on both efficiency (by increasing the contribution of stage leakage losses and secondary flow losses) and on manufacturability: for this reason the blades design has been optimized increasing as much as possible the aspect ratio by lowering the design flow coefficient (below the typical optimal values) but resulting in an overall maximized efficiency. Eventually a blades aspect ratio between 0.8 (first stage) and 0.9 last stage has been obtained.

The resulting rotating blades flow path is reported in the picture below:

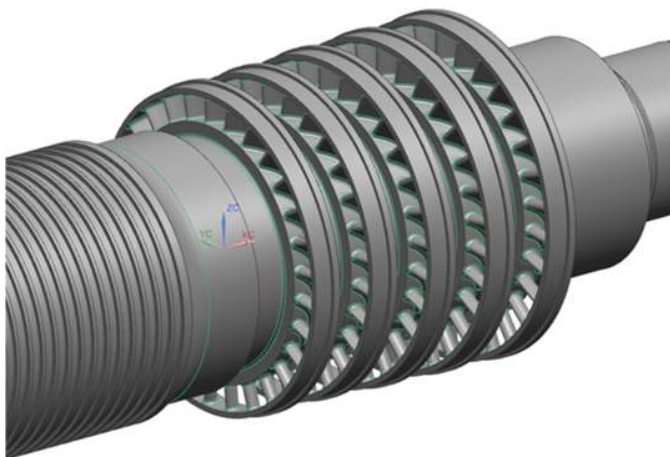


Figure 12: Rotor 3D Model

In order to maximize the turbine efficiency and especially to have a wider stable operating window, the first nozzle profile has been redesigned: as it is observable from Figure 13 there is an unnecessary flow overturning which has been fixed designing a dedicated airfoil.

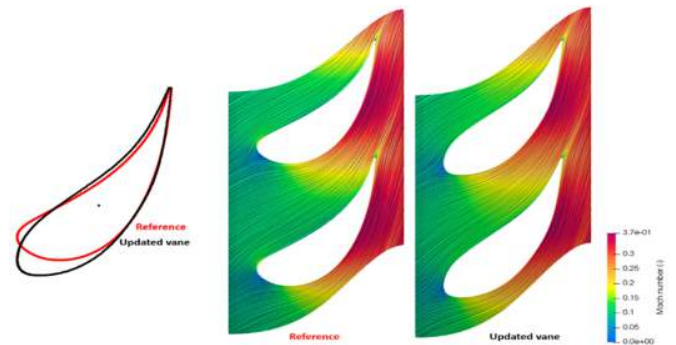


Figure 13: First stage nozzle re-design

Nozzles count selection have been done taking into account aeromechanical aspects: aiming to avoid any matching between mode shapes frequency with Blade passing frequency, or any low harmonic of the rotating speed (per-rev), which would have result in a resonance, each statoric row blades count has been selected to finalize an adequate frequency margin intersection as we can see from the SAFE diagram below (Figure 14) related to the 5th rotor: despite the turbine will operate at a constant speed, the diagram reports the harmonics of 95% and 105% speed to ensure, as previously mentioned, that no critical encroaches are present in the vicinity of the rated speed. As observable, integral design prevents any potential criticalities with low xREV (up to 27xREV) and 1xNPF and 2xNPF have been taken into account.

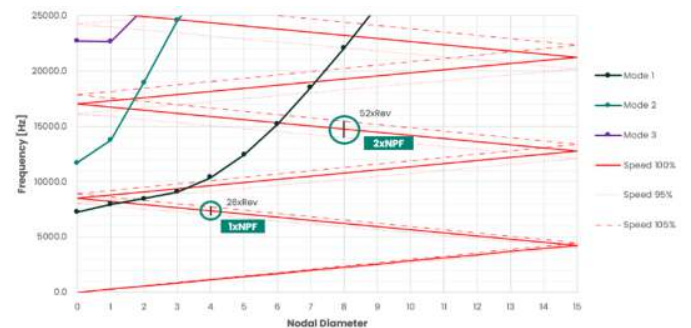


Figure 14: Stage 5 rotating blade safe diagram

Another important aspect inherent the flow path design was the interstage seals selection. The short blades developed for this application suffer tip clearance leakage losses even more than typical steam turbines challenging design so that it was extremely important minimize them as much as possible to optimize turbine efficiency. On the other hand, lowering radial clearances might results into rubbing due to rotordynamics criticalities: to handle both aspects at the same time, interstage spring seal has been adopted.

Mechanical verifications, both static and HCF ones, are typically performed with an internal OD tool which is based upon developed and proven data and correlations but considering that

this is an atypical design, dedicated FEM analyses have been carried out and in particular, as anticipated, deeper aeromechanical aspects have been studied to have a better understanding about fluid/structure interaction in such high density environmental on both flutter and HCF.

Lastly, performances and blades forced response have been verified with the adoption of a full 3D CFD unsteady state real gas calculation: the Figure 15 below shows an entropy plot taken at the midspan section of the entire turbine. More details about this work will be presented in a future conference.

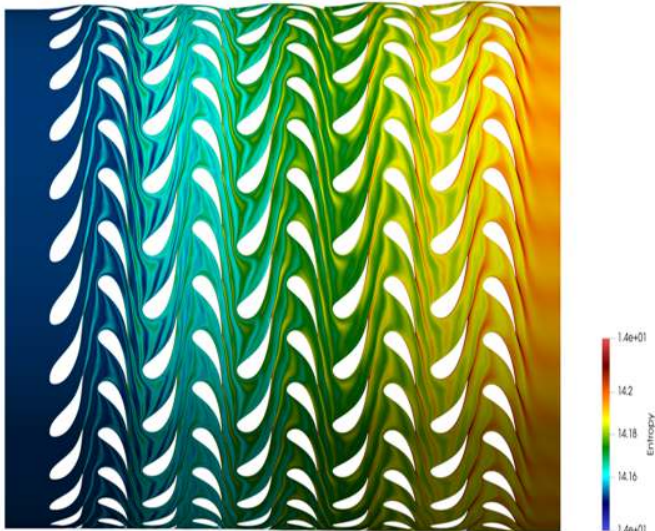


Figure 15: Full turbine 3D Unsteady CFD entropy plot

DRY GAS SEALS INTEGRATION AND THERMAL MODEL

As already mentioned in the introduction section, the design of a DGS cooling system is a crucial aspect for the expander design. Specifically, a cooling flow of 150 g/s for each DGS (0.55 % of the expander mass flow) is injected at 160 °C to maintain DGS below the maximum acceptable temperature. Most of the flow, after cooling the seal, is then reintegrated in the process, where it blends with balancing flow (2.2 % expander main flow) in front side and with flow-path main flow in rear side, as schematically explained in Figure 16.

The effectiveness of cooling system has been verified with a Whole Engine thermal Model carried out thanks to the findings proposed in a previous publication [24], in which a segregate conjugate heat transfer procedure has been presented and validated with experimental data provided by Flowserve on a sCO₂ DGS rotating test rig [25], readers can refer to these papers also for the DGS configuration. In addition to DGS maximum temperature verification, the thermal model is essential to investigate temperature gradients between hot region

of the expander, heated up by the main flow at 550-500 °C, and cold region of the expander, cooled to less than 250 °C by DGS and bearings cooling flow. This thermal behavior leads to the following thermal-structural challenges:

- High thermal stresses on the rotor in both the shaft-end regions, where strong temperature gradients are expected. These stresses can be mitigated by optimizing the location of the thermal transition region, obtaining an axial temperature gradient, and avoiding radial one.
- High thermal stresses on the head flange, which is averagely colder with respect to external casing, due to the DGS cooling flow. The head flange is indeed thermally coupled with external casing at the outer diameter and with DGS cartridge at the inner one.
- High radial differential displacement between head flange and DGS cartridge which adversely affects the design requirement of DGS energized seal which shall compensate radial misalignment between these components.

The steady-state expander temperature field as obtained after thermal optimization is reported in Figure 16.

In addition to the presented challenges associated with steady-state operating conditions, also the transient ones have been carefully investigated in this project by simulating the thermal model during entire expander mission, findings the following critical areas:

- High start-up pressure leads to strong flow-path heat transfer coefficient (e.g. 16000 W/m²K on rotor balancing drum) during start-up due to the fast metal temperature ramp of the rotor. The latter leads to high thermal stresses that can be reduced limiting sCO₂ inlet temperature during cold start-up.
- The DGS cooling shall be maintained in all the operating conditions, including expander and pump trip scenario, to shield the DGS from the heat flux coming via conduction from hot region of the expander. As a side effect, the cooling flow during expander trip can lead to fast forced cooling of hot regions near shaft-ends.
- During the start-up, it is essential to check cooling gas temperature in DGS to avoid phase-change due to expansion (Joule Thompson cooling effect). Concerning the last point, the expansion through the DGS has been investigated with p-H diagram (Figure 17) finding that in steady-state operating condition an injection temperature of 160 °C is sufficient to avoid phase change, still considering isenthalpic expansion (transformation A-B). The assumption of isenthalpic expansion is conservative since it neglects windage power transfer to fluid. The findings proposed in

previous works [24] [27] show how in full speed condition, isothermal expansion (transformation A-C) is the most suitable transformation to study this expansion. However, during start-up the rotational speed is reduced, and isenthalpic expansion shall be considered to conservatively check phase change. The p-h diagram shows how a minimum temperature above 80 °C (see A* point in Figure 17) is necessary to avoid phase change. At this purpose, a detailed CHT model of the DGS has been implemented.

ROTOR DESIGN

Rotor mechanical design is primarily driven by the following technical problematics: rotor-dynamic (both lateral and torsional), management of thermal stresses, axial thrust and overspeed. At extremely high level, when design an expander for sCO₂, all these aspects have some peculiarities which need to be properly addressed.

Some of the objectives are mutually conflicting and a design satisfying all of them must identify an acceptable tradeoff. From a qualitative standpoint, the major design conflicts, forcing multiple design iterations, can be summarized as follows:

- It has been already highlighted the need of a

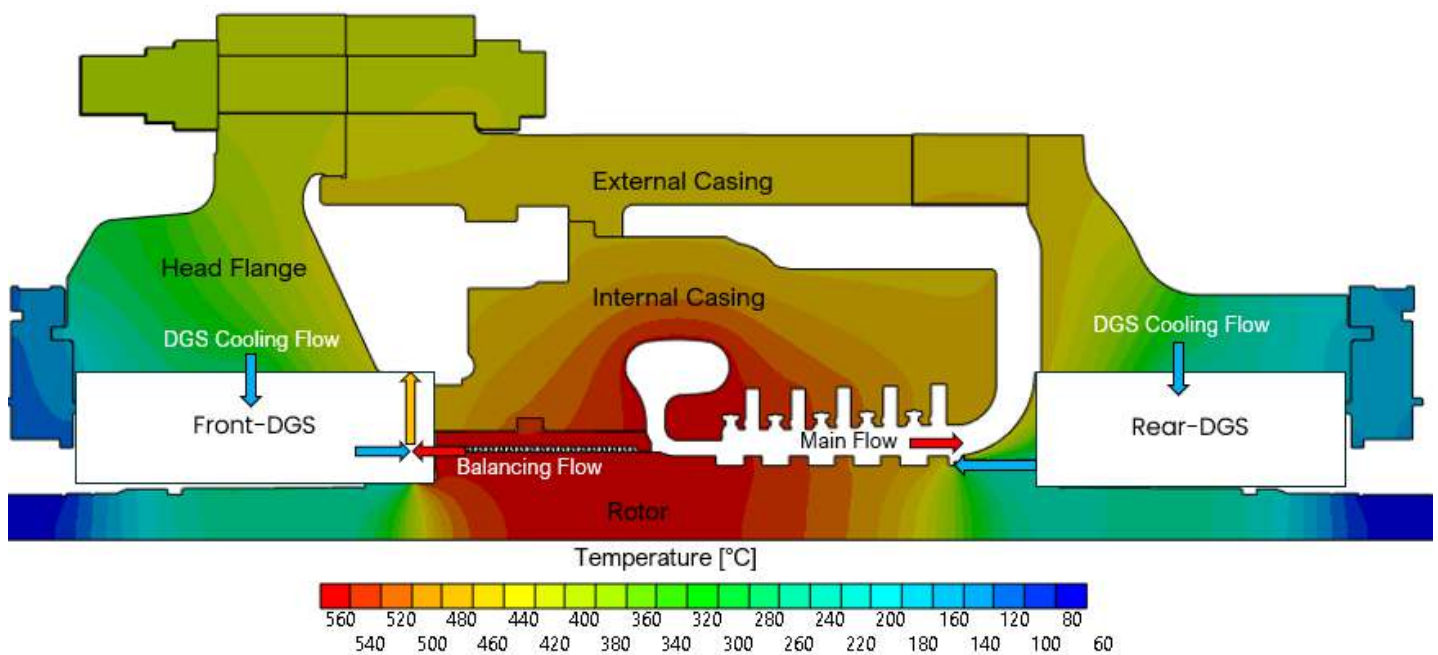


Figure 16: Full turbine temperature distribution plot

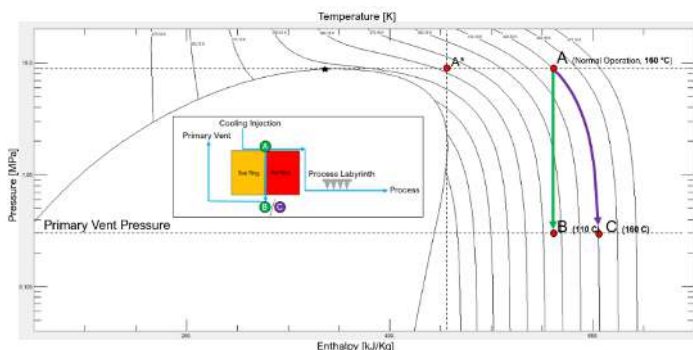


Figure 17: DGS Cooling flow pressure enthalpy diagram

cooling stream to maintain DGS within the allowable temperature limit: the effectiveness of the cooling must not exceed rotor thermal stresses consistent with its design life.

- The design options allowing to smooth the thermal stresses in the shaft end regions should avoid increasing the axial length of the thermal management region, since it is detrimental for the lateral stability.
 - The torsional sizing of the rotor can take advantage by the extremely low inertia characterizing sCO₂ rotors (0.135 kg*m² for Desolination): since the sizing in case of power generation applications is typically driven by the electrical malfunctioning torques (for steam turbines, for instance, short circuit or out-of-phase synchronization can easily result in 8-10 times the

nominal torque) more than by the torque driving the generator, having a low expander inertia allows to reduce the entity of those torques (as can be immediately derived by a rigid torsional analysis, as showed in [1]). Nevertheless, the downside of the reduced inertia is that the rotor must be capable to withstand an overshoot at the speed reached in case of loss of inertia (a coupling failure is an event that, although unlikely, is commonly considered in the industry when designing the rotor): the reduced inertia and the consequent large power-to-inertia ratio, results in overshoot speeds which are much larger if compared to other applications (steam turbines, for instance). For the Desolination case, it has been assessed that the rotor is able to withstand, with no burst failure, a momentary overshoot at >200% speed.

- Axial thrust by itself is not a challenge for sCO₂ expanders: the relatively low pressure-ratio imposed by the thermal cycles, usually not larger than 3-3.5, is such that sCO₂ flow-path can be designed with a cylindrical hub diameter or with a very small conicity. The balancing drum diameter necessary to compensate most of the thrust (down to a value allowable for the thrust bearing), hence, is not huge and, from the standpoint of the centrifugal stress, it does not represent a concern. The challenge that sCO₂ expanders have to face in terms of axial thrust is, primarily, the extreme sensitivity to the operating conditions either normal or abnormal: the high pressure application combined with the small diameter of the rotor (and, eventually, of the thrust bearing) is such that it is fundamental a very accurate prediction of the pressure all along the flow-path, in any design and off-design condition and, also, in any combination of internal clearances (both within the manufacturing tolerances or outside of them as a result of possible wearing of the inter-stage sealing).

In order to select a proper thrust bearing capable of withstand upon every possible operative condition, an analysis related to the worst-case scenario has been carried out and the following aspects have been considered as possible thrust uncertainty sources:

- EDM Manufacturing tolerances
- EoS uncertainty
- Statoric, rotoric and balancing drum clearances failure

With the purpose of being as conservative as possible, the worst scenario identified is with maximum pressure drop across the rotoric rows and minimum balancing pressure (which means the pressure upstream the 1st stage): this worst case

scenario has been achieved considering tolerances minimizing rotoric throat areas (which means tolerances taken positive at their maximum value) and maximizing the statoric ones (which means tolerances taken negative at their minimum value). Adopting the same philosophy we have considered that there could be a margined CFD discrepancy around $\pm 3\%$ due to equation of state uncertainty, maximizing the pressure drop along the rotors and minimizing it upon stators.

Lastly, in the evaluation of abnormal conditions, it has been considered any possible combination of clearances doubled with respect to the nominal value (for all the interstage seals and for the balancing drum one).

In conclusion, considering the extremely cautelative worst case scenario described above, there is an unbalanced maximum thrust approximately equal to 1750 kg which will be absorbed by the thrust bearing.

Table below reports thrust values for each case:

	CASES	THRUST [kg]
DESIGN POINT	-	200
WORST CASE SCENARIO	1	1755
BALANCING DRUM CLEARANCES DOUBLED	2	96
STATORS CLEARANCES DOUBLED	3	300
ROTORS CLEARANCES DOUBLED	4	-198
INTERSTAGES CLEARANCES DOUBLED	5	12
STATORS & BALANCING DRUM CLEARANCES DOUBLED	6	293
ROTORS & BALANCING DRUM CLEARANCES DOUBLED	7	-192
ALL CLEARANCES DOUBLED	8	1

Figure 17: Thrust values summary

The final outcome of the analysis involved in the rotor design is summarized here below.

Rotor-dynamic lateral stability is typically assessed by calculating the logarithmic decrement of the natural modes of concern: the first forward mode is, typically, the most critical one for this kind of rotor in “between the bearings” arrangement. The logarithmic decrement must be positive, with adequate margin, also when all the destabilizing effects are taken into account.

The main factor that can affect the rotor stability are the Alford effect and the seal’s effect. The Alford effect refers to the additional torque introduced by the non-circumferential uniform pressure distribution along the expander stages. The seal’s effect is due to the interaction between the fluid and rotor-stator surface that leads to additional energy to precession whirling (typically the forward one) able to increase the lateral amplitude vibration.

Rotor geometry (mass and stiffness) and dynamic coefficient of the bearings must be such that, when the destabilizing effects driven by the fluid are considered, a margin with respect to instability still applies.

The final rotor geometry, resulting after the multiple iterations necessary due to all the other design constraints, ended up over a calculated logarithmic decrement still positive when the destabilizing effects were included. Nonetheless, considering the uncertainties associated to the models calculating those destabilizing effects, the BH standard practice is to consider a multiplier factor that shall still result in a positive logarithmic decrement. Since the introduction of the multiplier did cause the disappearing of the stability margin, the solution finally pursued is to adopt journal bearings with Integral Squeeze Film Damping (ISFD). Such a bearing technology is extensively used to increase the damping in the rotor-bearing system, allowing also to fix cases where instability is experienced in running units.

In this case the idea is to keep ISFD as a backup margin, should it be necessary to correct abnormal rotor-dynamic behaviors at site: since these devices can be switched on in case that additional damping is necessary, the expander will be shipped with the ISFDs in locked configuration, so as to assess the stability with traditional tilting pad bearings.

The logarithmic decrement calculated including the multiplier factor into the destabilizing effects (according to the BH design practice) when ISFD bearing coefficients are used approaches 1.1 which according to the standard turbomachinery practice indicates a safe stability behaviour.

MATERIAL SELECTION AND COMPATIBILITY

Material selection has been one of the most crucial and toughest tasks encountered in the design of the expander. Material compatibility with pure CO₂ is widely addressed in the literature (a comprehensive review can be found, for instance, in [9]) but this is not the case of the Desolination working mixture.

Although the concept of CO₂ based mixtures was proposed, first, within the Scarabeus project (started before Desolination), materials have been more thoroughly assessed within Desolination, being the first opportunity to build a complete demonstration plant. As a matter of fact, the design of the expander for Scarabeus described in [1] has taken advantage by the preliminary results of the material compatibility tests carried out for Desolination: almost 2000 hours of exposure were cumulated when the Scarabeus design was published. At the moment of writing this paper, the compatibility tests have progressed but are still ongoing, hence no final results have been published in this regard and will neither be disclosed in this paper, considering also that there is a patent pending on this subject.

Here it is only remarked that, currently, the list of materials that cumulated an exposure comparable with the hours of operation planned for the Desolination demo (~2000 hours) has grown longer: initially, materials of interest for the major components (rotor and casings, driving the lead time of the expander) were tested. Subsequently, materials of interest for smaller components in contact with the process fluid (valves

internals, bolting, sensors...) have been tested too. The samples of the materials shortlisted for the major components have, currently, cumulated up to 4000 hours of exposure: even if durability in a real operational environment and in the longer term is still a question mark, the preliminary results of the compatibility tests allow to be confident that the materials under procurement will behave satisfactorily in the demonstration facility.

It is worth remarking also that the identification of suitable (or promising) materials for the process fluid has been an exercise other than obvious: although it is known that pure CO₂ at high temperature interacts with materials extensively used in turbomachinery design (like martensitic steels, that are prone to oxidation and carburization), there is a general consensus that Ni-based alloys experience much less interaction and are, generally, adequate for the application.

Conversely, some of the CO₂ based mixtures taken into consideration with the intent to shift up the critical temperature of pure carbon dioxide have been found extremely aggressive, even with respect to Ni-based alloys like Inconel 625 (see [10]): this is a fundamental reason that has forced, within the Desolination project, the working mixture shift from the original CO₂+C₆F₆ to the current CO₂+SO₂.

MANUFACTURING TECHNOLOGY

As highlighted in the technology challenge section, the low maturity of the manufacturing technology is revealing as one of the most critical hurdles in the whole Desolination expander development process. This issue has also been highlighted by the SwRI Step team at the latest ASME conference where the 740H piping fabrication experience has been illustrated in Cunningham et al. [26]). At the moment of this writing, the material selection of casing casting and rotor forging is under discussion because the lack of a qualified and competitive supply chain is triggering an extremely high cost (€/kg). Original selection foresees sand casting process for valves, external casing and inner casing and forging for the shaft. Rotating blades are made integral to the shaft (see Figure 18) leveraging EDM technology to create the blades passages into the solid shaft. This technology has already been successfully applied by Nuovo Pignone in the STEP rotor manufacturing. Selection of this solution is obviously favored by the specific small size of the Desolination expander but could be applicable to expander size up to at least 20 MW.



Figure 18: 3D Rotor complete model

As a solution to solve the above-mentioned supply chain issue, the possibility to adjust the cycle reducing the inlet temperature and eventually open to the adoption of commercially available materials like Inco625 is being explored. Specific compatibility tests at a lower temperature are being performed to demonstrate adequacy to the demonstrator test duration are also being performed.

CONCLUSIONS

The design and manufacturing of an sCO₂ expander for the Desolination EU funded project has been presented. Some critical design areas as the general architecture conception, Dry Gas Seals integration, the inlet hood aero optimization, the rotor design have been illustrated. Materials selection and manufacturing technology aspects have also been presented.

NOMENCLATURE

DGS:	Dry Gas Seals
LCF:	Low Cycle Fatigue
WEM :	Whole Engine thermal Model
BH:	Baker Hughes
EDM:	Electro Discharge Machining
CFD:	Computer Fluid Dynamics
SST:	Shear Stress Transport
ISFD:	Integral Squeeze Film Damper
Ψ :	Stage Load Coefficient
Φ :	Stage Flow Coefficient
C_x :	Stage Axial velocity
U:	Stage Peripheral Velocity

ACKNOWLEDGEMENTS

The project DESOLINATION have received funding from the European Union's Horizon 2020 research and innovation programme under grant agreements N°101022686. The authors gratefully thanks all the colleagues and University partners that have contributed to the completion of this project.

REFERENCES

- [1] Abdelrahman S., Paggini A., Diurno T., Martin T. White, Ruggiero M., Sayma A., (2022) *Integrated Aerodynamic and Mechanical Design of a Large-Scale Axial Turbine Operating With A Supercritical Carbon Dioxide Mixture*. Journal of Engineering for Gas Turbines and Power. February 2024
- [2] Marion J., Lariviere B., McClung A., Mortzhiem J., Ames R. *The STEP 10 MWe sCO₂ Pilot Demonstration Status Update*. ASME Turbo Expo 2020
- [3] Glos S., Lippe P., Schlehuber D., Kobler S., Wechsung M. (2021) *Design considerations of sCO₂ turbines developed within the carbosola project*. 4th European sCO₂ Conference 2021
- [4] Bidkar et al., *Conceptual Designs of 50MWe and 450MWe Supercritical CO₂ Turbomachinery Trains for Power Generation from Coal. Part 1: Cycle and Turbine*. The 5th International Symposium - Supercritical CO₂ Power Cycles 2016.
- [5] Crespi, F., Martínez, G., Rodriguez De Arriba, P., Sánchez, D. and Jiménez-Espadafor, F. *Influence of Working Fluid Composition on the Optimum Characteristics of Blended Supercritical Carbon Dioxide Cycles*. Turbo Expo: Power for Land, Sea, and Air. pp. V010T030A030.
- [6] Binotti, M., Marcoberardino, G. D., Iora, P., Invernizzi, C. and Manzolini, G. "SCARABEUS: Supercritical carbon dioxide/alternative fluid blends for efficiency upgrade of solar power plants." *AIP Conference Proceedings*. pp. 130002.
- [7] Morosini et al. *Preliminary characterization of the desolination project demo plant: design and off-design operability*. ASME Turbo Expo 2024
- [8] Moore et al. *Development and testing of a 10 MWe supercritical CO₂ turbine in a 1 MWe flow loop*. ASME Turbo Expo 2020
- [9] Oleksak, R. P., and Rouillard, F., 2020, "4.14 - Materials Performance in CO₂ and Supercritical CO₂," Comprehensive Nuclear Materials (Second Edition), R. J. M. Konings, and R. E. Stoller, eds., Elsevier, Oxford, pp. 422-451.
- [10] Putelli L. et al. *Preliminary Analysis of High-Temperature Corrosion of Metallic Alloys with CO₂ and CO₂-based Working Mixtures for Power Plants Applications* ASME Turbo Expo 2022, GT2022-8419
- [11] Muhammad, H. A., Lee, B., Imran, M., Cho, J., Cho, J., Roh, C., ... & Baik, Y. J. (2021). Investigating supercritical carbon dioxide power cycles and the potential of improvement of turbine leakage characteristics via a barrier gas. *Applied Thermal Engineering*, 188, 11660
- [12] Bidkar, R. A., Sevincer, E., Wang, J., Thatte, A. M., Mann, A., Peter, M., Musgrove, G., Allison, T., and Moore, J., 2017, "Low-Leakage Shaft-End Seals for Utility-Scale Supercritical CO₂ Turboexpanders," ASME J. Eng. Gas Turbines Power, 139(2), p. 022503.

- [13] Liao, X., Chalumeau, S., Crespi, F., Prieto, C., Lopez-Roman, A., Rodriguez de Arriba, P., ... & David, P. L. (2022, June). Life cycle assessment of innovative concentrated solar power plants using supercritical carbon dioxide mixtures. In *Turbo Expo: Power for Land, Sea, and Air* (Vol. 86083, p. V009T28A033). American Society of Mechanical Engineers.
- [14] Nielson, J., Kerr, T., Hellmig, B., Fesl, A., Laxander, A., & Philippi, P. (2022). Component Testing of a High Temperature Dry Gas Seal. In *The 7th International Supercritical CO₂ Power Cycles Symposium, San Antonio, TX, Feb* (pp. 21-24).
- [15] Cich, S. D., Moore, J. J., Day Towler, M., Mortzheim, J., & Hofer, D. (2019, June). Loop filling and start up with a closed loop sCO₂ Brayton cycle. In *Turbo Expo: Power for Land, Sea, and Air* (Vol. 58721, p. V009T38A006). American Society of Mechanical Engineers.
- [16] Thatte, A., & Dheeradhada, V. (2016, June). Coupled physics performance predictions and risk assessment for dry gas seal operating in MW-scale supercritical CO₂ turbine. In *Turbo Expo: Power for Land, Sea, and Air* (Vol. 49873, p. V009T36A017). American Society of Mechanical Engineers.
- [17] Thatte, A., Loghin, A., Martin, E., Dheeradhada, V., Shin, Y., & Ananthasayanam, B. (2016, March). Multi-scale coupled physics models and experiments for performance and life prediction of supercritical CO₂ turbomachinery components. In *The 5th international symposium-supercritical* (p. 1). Springer.
- [18] Fairuz, Z. M., & Jahn, I. (2016). The influence of real gas effects on the performance of supercritical CO₂ dry gas seals. *Tribology International*, 102, 333-347.
- [19] Trivedi, D., Bidkar, R. A., Wolfe, C., & Zheng, X. (2018, June). Film-stiffness characterization for supercritical CO₂ film-riding seals. In *Turbo Expo: Power for Land, Sea, and Air* (Vol. 51098, p. V05BT15A023). American Society of Mechanical Engineers.
- [20] Trivedi, D., Bidkar, R. A., Wolfe, C. E., & Mortzheim, J. (2019, June). Supercritical co₂ tests for hydrostatic film stiffness in film-riding seals. In *Turbo Expo: Power for Land, Sea, and Air* (Vol. 58721, p. V009T38A018). American Society of Mechanical Engineers.
- [21] Tallman, J. A., & Bidkar, R. A. (2018, June). Heat transfer coefficient characterization for large aspect-ratio thin films in film-riding seals. In *Turbo Expo: Power for Land, Sea, and Air* (Vol. 51098, p. V05BT13A009). American Society of Mechanical Engineers.
- [22] Zakariya, M. F., 2018, "Simulation and Development of Dry Gas Seal for Supercritical CO₂ Carbon Dioxide," Ph.D. thesis, University of Queensland, Brisbane, Australia.
- [23] Wilkes, J., Robinson, K., Wygant, K., Pelton, R., & Bygrave, J. (2022, June). Design and testing of a 275 bar 700 degree celsius expander for an integrally geared supercritical co₂ compander. In *Turbo Expo: Power for Land, Sea, and Air* (Vol. 86083, p. V009T28A025). American Society of Mechanical Engineers.
- [24] Rafanelli, I., Generini, G., Andreini, A., Diurno, T., Girezzi, G., & Paggini, A. (2024). Development and Validation of a Segregated Conjugate Heat Transfer Procedure on a sCO₂ Dry Gas Seal Test Bench. *Journal of Engineering for Gas Turbines and Power*, 146
- [25] Steinmann, D., Kassimi, R., Kleiner, J., Susini, P., Milani, A., & Dozzini, M. (2022). Dry gas seals design for centrifugal compressors in supercritical CO₂ application. 7th International sCO₂ Power Cycles Symposium San Antonio, Texas.
- [26] Cunningham S. et al. (2024), The Design, Fabrication, and Installation of the Inconel 740H Piping System for a 10 MW sCO₂ Pilot Plant. In *Proceedings of ASME Turbo Expo 2024*
- [27] Laxander, Armin. "Development and testing of dry gas seals for turbomachinery in multiphase CO₂ applications." (2019).

DuEPublico

Duisburg-Essen Publications online

UNIVERSITÄT
DUISBURG
ESSEN

Offen im Denken

ub | universitäts
bibliothek

Published in: 6th European Conference on Supercritical CO₂ (sCO₂) for Energy Systems

This text is made available via DuEPublico, the institutional repository of the University of Duisburg-Essen. This version may eventually differ from another version distributed by a commercial publisher.

DOI: 10.17185/duepublico/83281

URN: urn:nbn:de:hbz:465-20250428-104914-7



This work may be used under a Creative Commons Attribution 4.0 License (CC BY 4.0).